COMPUTATIONAL ANDSTRUCTURAL BIOTECHNOLOGY JOURNAL

Single-Component Bismuth Nanoparticles as a Theranostic Agent for Multimodal Imaging-Guided Glioma Therapy

Shu-Ting Lu [a], Dan Xu [b], Ru-Fang Liao [a], Jia-Zhen Luo [a], Yu-Hang Liu [a], Zhen-Hua Qi [a], Cai-Ju Zhang [a], Nai-Li Ye [a], Bo Wu [a,*], Hai-Bo Xu [a,*]

[a] Department of Radiology, Zhongnan Hospital of Wuhan University, Wuhan University, Wuhan 430071, PR China
[b] Department of Nuclear Medicine, Zhongnan Hospital of Wuhan University, Wuhan University, Wuhan, 430071, PR China

ARTICLE INFO

ABSTRACT

Single-component nanomaterials such as bismuth (Bi) based on nanoparticles (NPs) intrinsically having both diagnostic and therapeutic capabilities are widely needed in biomedical fields. However, their design and fabrication still face enormous challenges. Here, a kind of pure Bi NPs with ultrahigh X-ray attenuation coeffcient was developed and evaluated as a simple but powerful theranostic nanomaterals and potent light-to-heat conversion efficiency for photoacuostic imaging (PAI)/photothermal therapy (PTT) in this study. The prepared pure Bi NPs showed excellent photothermal performance and the temperature of NPs solution (1 mg/mL) increased to 70 °C under near-infrared light irradiation within 4 min. The pure Bi NPs showed obvious enhancement effect both in X-ray computed tomography (CT) and PA imaging modalities *in vivo*. In addition, the glioma growth was efficiently suppressed by the pure Bi NPs after 808 nm laser irradiation, while maintained the biosafety and low toxicity. Thus, it is notable that this type of Bi nanomaterial has great potential in multi-imaging guided cancer treatment.

1. Introduction

Recent advances in nanotechnology have profoundly affected the biomedical research. Research on PTT based on multifunctional nanomaterials is a rapidly growing field and offers unprecedented opportunities to improve cancer therapy. PTT based on light absorbing agents to realize localized destruction of cancer cells by conversion of light into heat [1–4]. As a non-invasive therapeutic technique, PTT has many advantages such as improved selectivity, remoted controllability, and low systemic toxicity compared with conventional methods [5]. Unlike chemotherapy, PTT has different therapeutic mechanisms and could avoid drug resistance of cancer cells. Specifically, PTT utilizes nanoparticles embedded within tumors as exogenous energy absorbers to convert laser light energy into heat to ablate cancer cells. Compared with other biological macromolecules, proteins have higher abundance and lower stability. And high heat can induce the protein denaturation, which can result in cancer cell death [6,7]. Imaging-guided PTT combines diagnostic imaging and therapy through novel biomaterials such as multifunctional nanomaterials [8]. It provides researchers' capabilities to diagnose disease, monitor therapeutic response, guide procedures and make cancer treatment with high specificity and sensitivity [9,10].

Due to the high spatial resolution and short image acquisition time., many clinic imaging modalities, X-ray computed tomography (CT) is becoming one of the most efficient and powerful techniques for tumor diagnosis, Among many clinic imaging modalities, X-ray computed tomography (CT) is becoming one of the most efficient and powerful techniques for tumor diagnosis, due to the high spatial resolution and short image acquisition time. Specifically, CT has attracted much attention because of its high resolution for locating tissues of interest. While CT has low sensitivity in differentiating between complex soft tissue structures. Recently, PAI emerges as a new biomedical imaging technology based on the use of laser-generated thermal expansion and ultrasound. [11,12] Compared with conventional optical imaging techniques, PAI allows deeper tissue detection and offers higher spatial resolution and it can obtain multiscale imaging of living biological structures ranging from organelles to tissue [13,14]. In contrast with CT, PAI has excellently high sensitivity in presenting soft tissue, which can visualize tissue functions and diseases. Thus, it would be highly desired to combine CT with PAI techniques which could make full use of each advantages and characters,especially in better diagnosing and locating of cancerous tissue while at the same time avoiding the shortcomings of both. The PAI/CT bimodal imaging may provide the improved precision, feasibility and efficacy of diagnosis [15,16]. Further combination of PAI/CT with PTT

* Corresponding authors.
 E-mail addresses: wubo5317@whu.edu.cn (B. Wu), xuhaibo@whu.edu.cn (H.-B. Xu).

could realize theranostic and image guided treatment of diseases. However, the practical applications of current theranostic agent such as polymer-inorganic hybrid nanoparticles (NPs), metal doped NPs [17], liposomes [18], and mesoporous SiO_2 NPs [19] have been largely limited due to the complicated synthesis, increased toxicity and instability. Therefore, single-component nanomaterials such as inorganic nanoparticles intrinsically having both diagnostic and therapeutic capabilities are much more desirable.

The current available inorganic theranostic nanoparticles for CT mainly comprise of metal elements with high atomic number, such as Au- [20], Pt- [21], Ta- [16], or Bi- [22] based nanomaterials, which have been indicated to improve the sensitivity and diagnostic time window in these years. It has been reported that Bi-based NPs can be employed in CT enhancement imaging for many years, owing to its'largest atomic number and high X-ray absorption efficiency of Bi element among the "nonradioactive elements" [23,24]. Additionally, Bi element has good biocompatibility and low toxicity, which has been proven through the widely used drugs contained Bi element in clinical therapy. For example, ranitidine bismuth citrate (RBC, Pylorid, Tritec) has been served as conventional method to eradicate Helicobacter pylori [25,26]. Compared with the other heavy mental elements, Bi is the cheapest element, whichsuit to further use in many biomedical areas including CT contrast imaging. Meanwhile, Bi-based NPs with narrow direct bandgap exhibited strong near infrared (NIR) absorbance, which demonstrated a great potential in PAI and PTT [27–30]. Therefore, several Bi-based nanomaterials, such as Bi_2S_3 and Bi_2Se_3 nanostructures [23,31], have been synthesized and evaluated for CT, PAI and PTT [27]. For example, Bi-NPs, specifically, Bi_2S_3 nanorods have been reported as a competent PTT agent for the first time by Liu et al. [10] Subsequently, Li et al. reported a highly porous PEGylated Bi_2S_3 nano-urchins that demonstrated high performance for effective PTT guided by CT and PAI and infrared thermal (IRT) triple-modal imaging [32]. However, both studies have been focused on the structure design based on bismuth sulfuret. The research on developing pure Bi-NPs suitable for cancer PAI and PTT was quite few. Inspired by the excellent performance of Bi_2S_3 nanomaterials in PTT [32,33], the pure Bi-NP was developed and evaluated as a simple but powerful theranostic nanomaterial for PTT/PAI/CT in this study.

In this study, we presented the development of [polyethylene glycol-2000]-2-distearoyl-sn-glycero-3-phosphoethanolamine DSPE-PEG) coated pure Bi-NPs (DSPE-PEG-Bi NPs), which served not only as a potential CT contrast agent, but also an excellent PAI and PTT agent. The results *in vitro* and *in vivo* indicated the satisfactory contrast effect in CT and PAI imaging and excellent light-to-heat conversion efficiency of DSPE-PEG-Bi NPs. Meanwhile, the DSPE-PEG-Bi NPs showed great biocompatibility, low toxicity and stability. These results made DSPE-PEG-Bi NPs promising theranostic agents for CT/PAI imaging and PTT therapy (Scheme 1).

## 2. Materials and Methods

2.1. Materials

1,2-Distearoyl-sn-glycero-3-phosphoethanolamine-N-[methoxy (polyethylene glycol)-2000] (DSPE-PEG2000) and 1, 2-distearoyl-sn-glycero-3-phosphocholine (DSPC) was purchased from Shanghai Advanced Vehicle Technology Co., Ltd. $Bi(NO_3)_3 \cdot 5H_2O$ was purchased from Sigma-aldrich (Shanghai, Trading Co., Ltd). 1-dodecanethiol (DT) was purchased from Aladdin Reagent Co., Ltd. All reagents were of analytical grade and used without further purification. Iopromide, cyclohexane and ethanol were purchased from Sinopharm Chemical Reagent Co., Ltd. The consumables of cell culture in this work and fetal bovine serum (Scitecher) were purchased from Beijing Dingguo Changsheng Biotechnology Co., Ltd.

2.2. Synthesis of Hydrophobic Dodecanethiol-Bi Nanoparticles (DT-Bi)

All $Bi(NO_3)_3 \cdot 5H_2O$ (970 mg) were added to the three neck flask with 1-dodecanethiol (10 mL) under magnetic stirring and nitrogen protection. The reaction was heated 178 °C for 1 min and a clear black solution was obtained. After cooling to 40 °C at room temperature, the product was centrifuged and washed for 3 times (8000 rpm, 15 min) with absolute ethyl alcohol to remove any possible remnants. Then, the sediments were dissolved in cyclohexane and centrifuged (6000 rpm, 10 min). The final DT-Bi nanoparticles were dispersed in cyclohexane for future use.

2.3. Preparation of DSPE-PEG-Coated Bi Nanoparticles (DSPE-PEG-Bi NPs)

The DSPE-PEG-Coated Bi nanoparticles with water-solubility and good biocompatibility were prepared using a self-assembly method. Briefly, 75 mg DSPE-mPEG (2000), and 50 mg DSPC were dissolved in 20 mL 4 wt% phosphate buffer saline (PBS). Then 10 mL cyclohexane solution with 100 mg DT-Bi nanoparticles were absolutely mixed *via* a microtip probe sonicator at 30 W output under natural condition. After that, the solution was vortexed at 45 °C for about 3 h to completely vaporize the cyclohexane. Finally, the DSPE-PEG-Bi NPs solution was filtered through a 0.22 μm filter in order to remove large aggregates for the following experiments. Inductively coupled plasma mass
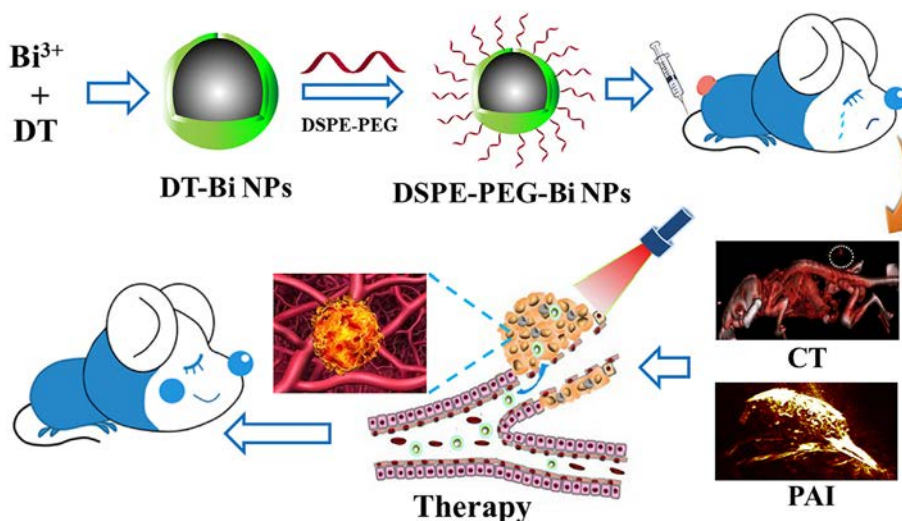
Scheme 1. Schematic illustration of DSPE-PEG-Bi NPs for CT/PA imaging and therapy.

spectrometry (ICP-MS) data showed that the as-prepared solution had amount of Bi element.

2.4. Characterization

The polydispersity index (PDI) of the DT-Bi NPs and DSPE-PEG-Bi NPs was measured by Zetasizer Nano ZS (DLS, Malvern Instruments Ltd., UK) with a He—Ne laser beam (633 nm). The morphologies and microstructures of the products were observed by field emission transmission electron microscopy (TEM, JEM-100CXII 100 kV) Fourier transform infrared spectra (FTIR) of the NPs was obtained by a Nicolet IS 10 spectrometer (Thermo Scientific, Madison, WI). The X-ray photoelectron spectra (XPS) under an Al Kα X-ray source were detected by an ESCALAB 250Xi system (Thermo Scientific). The UV absorption spectra were collected using a Hitachi U-3900 spectrophotometer.

2.5. Cells and Animals

The rat glioma cells (C6 cells) and African green monkey SV40-transformed kidney fibroblast cells (COS-7) were obtained from the China Center for Type Culture Collection (Wuhan University) and cultured in DMEM with 10% FBS at 37 °C to future use. Female BALB/c nude mice with about 5–6 weeks old were pursued from Beijing HFK Bioscience Co. Ltd. All mice were placed in the standard pathogen-free conditions (60% relative humidity, 20 °C room temperature). After acclimating 5 days, animals were subcutaneously injected with around 2×10^6 C6 cells for each mouse. All the experiments were conducted following the local animal care and use ethics committee.

2.6. In Vitro and In Vivo Photothermal Profile

In order to assess the photothermal profile of DSPE-PEG-Bi NPs in vitro and in vivo, the temperature was measured by the infrared imaging system. In vitro, 1 mL DSPE-PEG-Bi NPs solution (1 mg/mL) was capped and wrapped with parafilm air-tightly to avoid the possible solvent evaporation, and then illuminated with various power densities of NIR laser (1.5, 1.0, 0.5 W/cm^2). In vivo, DSPE-PEG-Bi NPs (10 mg/mL, 200 μL) or PBS (200 μL) was injected into tumor-bearing mice by tail vein. After 1 h injection, with 808 nm laser irradiation at a power density of 1 W/cm^2, the temperature of tumor sites was recorded with infrared imaging system (IR thermo-camera systems, FLIR A35, FLIR Systems, Inc., USA) at different time intervals.

2.7. Cell Viability Assay

To evaluate the cytotoxicity and the photothermal therapy effect of Bi NPs in vitro, the MTT assay was studied. Firstly, about 4×10^3 cells were seeded in each well of a 96-well plate with the DMEM medium containing 10% fetal bovine serum (FBS) at 37 °C. After 24 h incubated, the adherent C6 cells and Cos-7 cells were observed by microscope and co-incubated with different concentration of DSPE-PEG-Bi NPs (6.25, 12.5, 25, 50, 100 and 200 μL) for another 24 h. After 24 h co-incubated, the C6 cells were removed the medium with or without laser irradiation at 1 W/cm^2 for 10 min. The untreated cells were negative control group. After that, 100 μL of fresh medium with 10 μL MTT (0.5 mg/mL) were added into each well for 4 h. Then the supernatant was completely removed and 150 μL of DMSO was replaced to measure the cell viability via microplate reader at 570 nm.

2.8. Live-Dead Staining In Vitro

Approximately a density of 5×10^5 C6 cells were seeded in each well of 6-well plates with overnight incubated. Then the 0.2 mg/mL of DSPE-PEG-Bi NPs solution were added in two wells and the rest wells added PBS for 12 h. After 12 h co-incubation, the medium was absolutely removed and applied a 808 nm laser irradiation at 1 W/cm^2 to 6-well plates for 10 min. The C6 cells were washed by PBS for 3 times and collected to dye with Calcein-AM/PI Double Stain. Then they were observed the live cells (green) and the dead cells (red) by confocal microscopy. The wells were received irradiation only and PBS only for control groups.

2.9. In Vitro CT and PA Imaging

For evaluating the contrast efficiency of the different concentration of DSPE-PEG-Bi NPs, the CT and PA imaging in vitro were studied. For CT imaging, different concentration of DSPE-PEG-Bi NPs and Iopromide solutions (20, 15, 10, 5 and 0 mg/mL) were placed on a 96-well plate and were scanned by clinical X-ray CT (Siemens, Definition AS) to obtain the CT map and CT value. The CT imaging parameterswere as follows: slice thickness 154 μm, field of view (78.92 mm–78.92 mm), effective pixel size 50 μm, tube voltage 80 kV, tube current 270 μA.

For PA imaging, Bi NPs solutions at different concentrations (10, 5, 2.5, 1.25, 0.625 mg/mL) were filled into glass pipes. And the PA images and PA signal value were collected by a PA system (Endra Nexus 128).

2.10. In Vivo CT and PA Imaging

To evaluate the tumor imaging of different time point in vivo, the C6 tumor-bearing mice (n = 3) were intravenously injected DSPE-PEG-Bi NPs solution (200 μL, 10 mg/mL) until all tumors grew up to a volume between 100 and 400 mm^3. For in vivo CT imaging, before and after 0.5, 1 and 3 h of the intravenously injection, imaging were taken by on clinical X-ray CT (Siemens, Definition AS). Then, the CT value of tumors' region and the 3D reconstruction maps were obtained via the own post-processing software.

The PA imaging studies started before and after 0.5, 1 and 3 h injected, all imaging and PA signal value were collected by a PA system (Endra Nexus 128) with different excitation light wavelengths (680–900 nm). During CT and PAI scanning, all mice (n = 3) were under anesthesia by isoflurane. For scanning in vivo, the scan parameters were the same as in vitro.

2.11. In Vivo Photothermal Cancer Therapy

The photothermal cancer therapy studies were performed on C6 glioma tumor models. When the tumor volume was about 50 mm^3, 16 tumor-bearing mice were divided into 4 groups (n = 4). For the treatment group, 200 μL of 10 mg/mL DSPE-PEG-Bi NPs solution was intravenously injected for the first time. After 1 h injection, the whole region of tumor was irradiated by 808 nm laser at density of 1 W cm^{-2} for 10 min. The 3 control groups were possessed: 1) irradiation only (1 W/cm^2, 10 min), 2) PBS only (200 μL), 3) Bi NP solution only (200 μL, 10 mg/mL). During the whole therapy, the body weight and the tumor volume were measured every other day for 12 days. And the volume was calculated by following the formula: $V = L \times W^2/2$, (L stands for the length, W stands for the width). After 12 days, the tumors and the organs (heart, liver, spleen, lung and kindey) were dissected for hematoxylin and eosin (H&E) stains.

2.12. Liver Function and Blood Analysis

The tumor-bearing mice (n = 3) were injected 200 μL DSPE-PEG-Bi NPs (10 mg/mL). At the various times (0, 1, 12, 24, 48 and 72 h), 150 μL bloods were collected for liver function (Icubio, iMagic-V7), and blood biochemical indexes were measured by Auto Hematology Analyzer (MC-6200VET).

2.13. Statistical Analysis

All experimental data are presented as mean ± SEM. As shown in Figs. 4a and 6b and c, the statistical differences were determined by

S.-T. Lu et al. / Computational and Structural Biotechnology Journal 17 (2019) 619–627

two-sample/group *t*-test. Student-Newman-Keuls was used in Fig. 6a. P < .05 was considered statistically significant.

3. Discussion and Results

3.1. Preparation and Characterization of DSPE-PEG-Bi NPs

In order to obtain the DSPE-PEG-Bi NPs with narrow size distribution, the ultrasonic emulsification method was used to prepare DSPE-PEG-Bi NPs. Firstly, two reactants of ($Bi(NO_3)_3$ and 1-dodecanethiol (DT)) were employed to obtain DT-Bi NPs by using a facile non-injection method. As shown in Fig. 1a, the results of typical TEM image demonstrated that the DT-Bi NPs exhibited a uniform size with spherical shape in cyclohexane. To further make them dispersed individually in aqueous solution and to improve their biocompatibility, a ultrasonic emulsification method was employed to coat DT-Bi NPs with an amphipathic PEG surfactant DSPE-PEG2000. DSPE-PEG is a kind of amphiphilic polymer used extensively for improving blood circulation and biocompatibility of variety of NPs. As shown in Fig. 1b, the diameter of DSPE-PEG-Bi NPs was 105 nm after modification, which is suitable for *in vivo* application since it has been recognized that NPs with diameter size ranging from 100 to 200 nm have prolonged circulation half-life in the blood, and thus helping them to home in tumor by enhanced permeation and retention (EPR) effect [34]. In addition, the successful functionalization of DT-Bi NPs with DSPE-PEG was also confirmed by TEM (Fig. 1d). Especially the modified DSPE-PEG-Bi NPs displayed excellent monodispersity in PBS (Fig. 1e). The UV–vis-NIR absorption curve demonstrated that as-prepared DSPE-PEG-Bi NPs exhibited a wide absorption (Fig. 1e). The FTIR and XPS results were used to prove the successful coating of DSPE-PEG on DT-Bi NPs, and these proofs have been discussed in the revised manuscript. The formation of paramagnetic layer on the surface of Bi NPs was confirmed from the characteristic bands of DSPE-PEG in the 1639 (CO, amide I), 2921, 2852 (CH alkyl) in the FT-IR spectra (Fig. 1c). The result of XPS was showed in the Fig. 1f. The characteristic peaks of Bi (159.1 eV, Bi 4f) could be found in the XPS spectrum of the DSPE-PEG-Bi NPs, which confirmed the existence of Bi on nanoparticles.

3.2. In Vitro and In Vivo Photothermal Profile

The NPs contained Bi element has been proven to have efficient NIR photothermal conversion ability. Here, the photothermal effect of the pure Bi NPs was evaluated though the experiments *in vitro* and *in vivo*. As presented in Fig. 2a, photothermal imaging recorded a rapidly increase in the temperature of DSPE-PEG-Bi NPs solution (1 mg/mL) for 1 min of 808 nm laser irradiation at the power density of 1.0 W/cm². After 4 min irradiation, the temperature increased nearly 40 °C, while the temperature of PBS increased byonly about 0.5 °C. As shown in Fig. 2b, when the power density rose to 1.5 W/cm², the temperature of DSPE-PEG-Bi NPs had a higher increase to 76.6 °C for 4 min. In addition, after the temperature of DSPE-PEG-Bi NPs (1 mg/mL) reached the maximum with irradiation, the temperature decreased slowly to the nature condition without irradiation. Besides, this process could be repeatable (Fig. 2c). To further examine the PTT effect of DSPE-PEG-Bi NPs in living animals, the tumor region of tumor-bearing mice accepted 10 mg/mL i.v injection was irradiated by 808 nm laser. As shown in Fig. 2e, the PTT imaging and the temperature of tumor region were collected by an infrared camera. The tumor region of treatment group was clearly lightened with the time increased. As presented in Fig. 2d, comparing with the control group, the temperature at tumor region rose from 26.1 to 48.8 within 5 min, which could inhibit the growth of tumor efficiently. These findings proved that the DSPE-PEG-Bi NPs had excellent PTT effect, which enabled to induce hyperthermia to kill tumor.
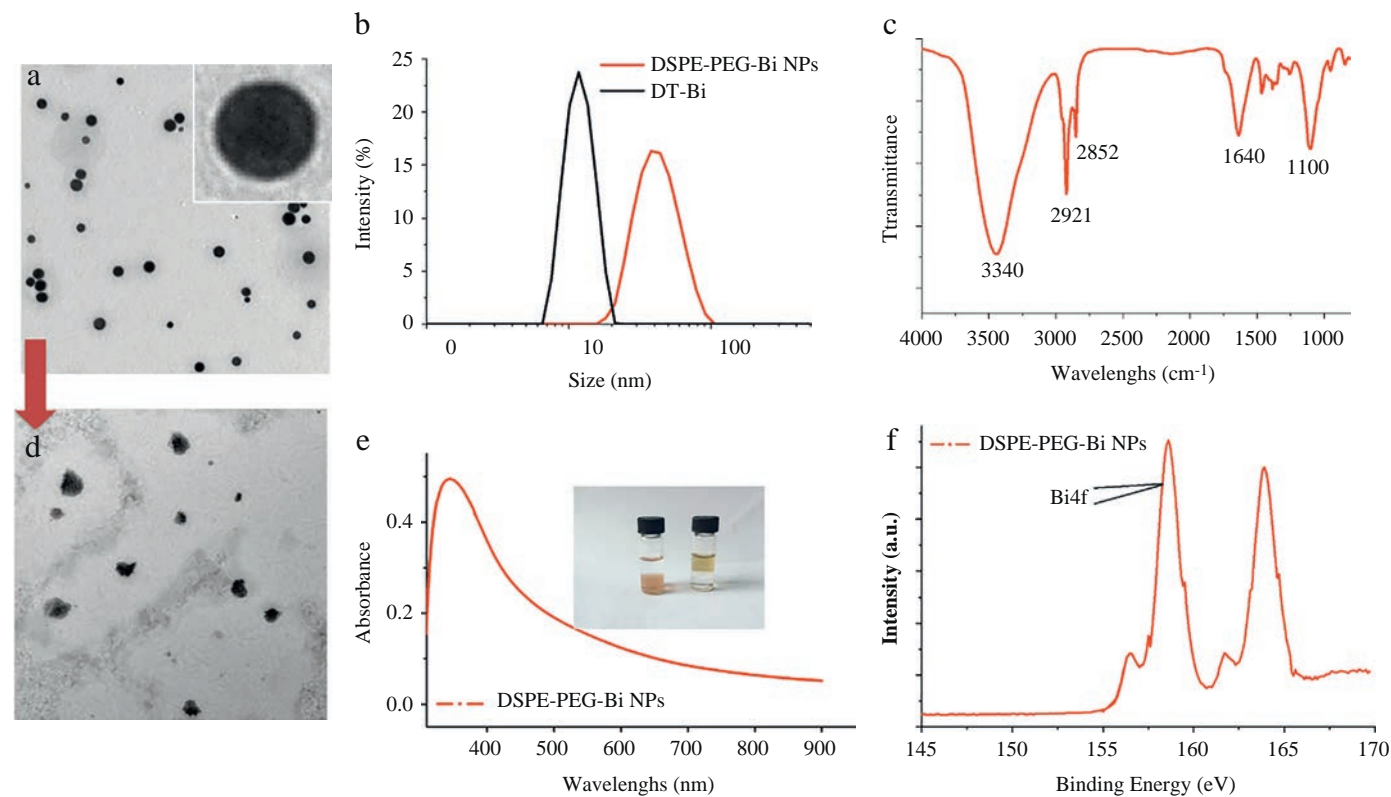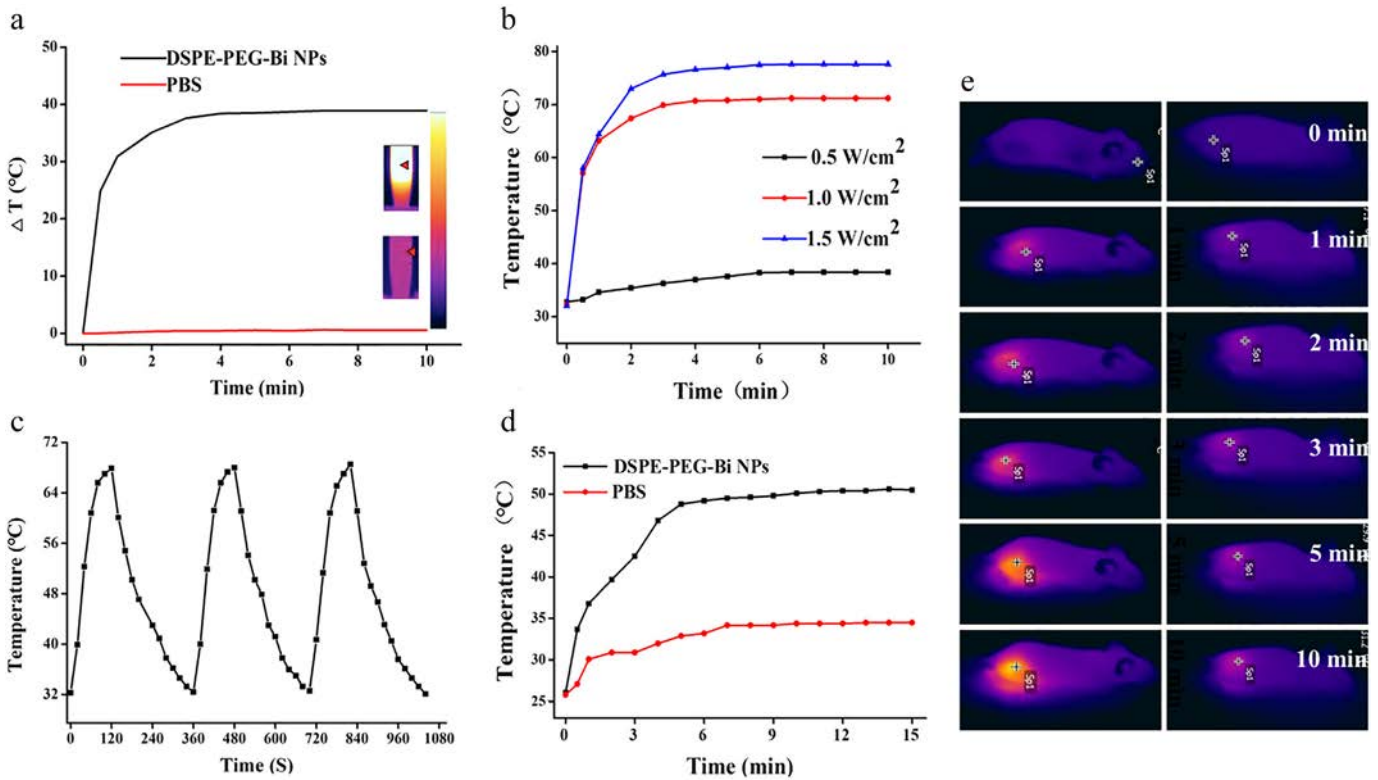

Fig. 1. a) TEM images of as-prepared DT-Bi NPs. b) Dynamic light scattering of DT-Bi and DSPE-PEG-Bi NPs. c) FT-IR spectra of DSPE-PEG-Bi NPs. d) TEM images of DSPE-PEG-Bi NPs. d) UV–vis absorbance spectra of DSPE-PEG-Bi NPs (Inset in Fig. d): photo of DSPE-PEG-Bi NPs solution in deionized water (left); DT-Bi NPs solution in cyclohexane (right). f) XPS spectra of DSPE-PEG-Bi NPs.

Fig. 2. a) photothermal effect of DSPE-PEG-Bi NPs (1 mg/mL), and the illustration under the right indicated the PT imaging of DSPE-PEG-Bi NPs (up) and PBS (down) after 10 min irradiation (1.0 W/cm^2). b) Temperature variation curves of DSPE-PEG-Bi NPs (1 mg/mL) under 808 nm laser (0.5, 1.0 and 1.5 W/cm^2) irradiation. c) Temperature curve of DSPE-PEG-Bi NPs (1 mg/mL) with repeated irradiation (1 W/cm^2) on/off cycles. d) The temperature of tumor region and e) the PT imaging of mice with (left) or without (right) DSPE-PEG-Bi NPs under 808 nm laser (1.0 W/cm^2) irradiation.

3.3. The CT and PA Imaging In Vitro

With largely atomic number and X-ray absorption coefficient, bismuth-based nanomaterials have been proven to be a good CT contrast agent [35,36]. Therefore, after synthesizing DSPE-PEG-Bi NPs with good biocompatibility, CT contrast efficacy of DSPE-PEG-Bi NPs was assessed. The CT imaging and CT value *in vitro* with different concentrations of DSPE-PEG-Bi NPs were firstly collected through a clinic CT. As shown in the CT imaging *in vitro* (Fig. 3c), obvious lightening effect was observed at the higher concentration of DSPE-PEG-Bi NPs,
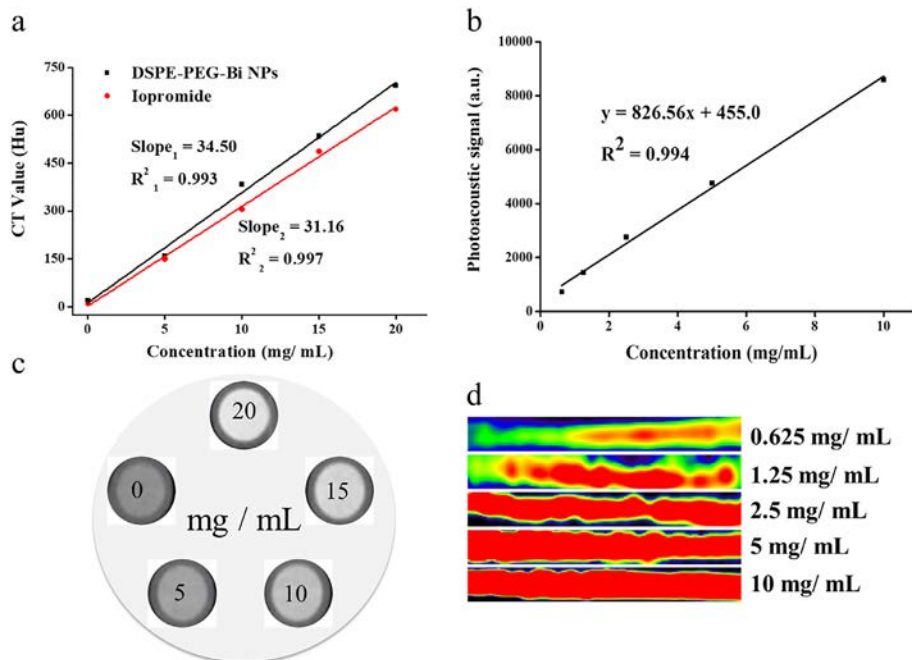

Fig. 3. a) CT values (HU) of DSPE-PEG-Bi NPs and Iopromide at different concentrations. b) PAI signal values of DSPE-PEG-Bi NPs with different concentrations. c) *In vitro* CT images and d) *In vitro* PA images of DSPE-PEG-Bi NPs at different concentrations.

which could be a beneficial consequence of the high X-ray absorption coefficient of Bi element. Meanwhile, the CT values (Hounsfield units, Hu) of DSPE-PEG-Bi NPs increased linearly and the slope was 34.50 ($R^2 = 0.993$), which was higher than Iopromide (31.16) commonly used in the clinic. As shown in Fig. 3a, the CT value of DSPE-PEG-Bi NPs was much higher than the same concentration of Iopromide. For example, the CT value was 693.94 for 20 mg/mL DSPE-PEG-Bi NPs, while Iopromide was about 619.77. The results demonstrated that DSPE-PEG-Bi NPs with 100% content of Bi element is a satisfactory CT contrast agent.

As a kind of noninvasive biomedical imaging, PAI can be used to obtain the deeper tissues with higher spatial resolution. The above characterization results demonstrated the high NIR absorption of DSPE-PEG-Bi NPs, which indicated the potential of DSPE-PEG-Bi NPs in PAI enhancement. To further investigate the PAI enhancement efficacy, various concentrations of DSPE-PEG-Bi NPs were prepared for PAI imaging in vitro. As shown in Fig. 3b, the contrast effect of PAI was increased with its concentration, which was similar to the effect of CT. What's more, strong PAI signals were detected even at the lowest concentration of DSPE-PEG-Bi NPs. For the PA signal values (Fig. 3d), there was obviously linear relationship ($R^2 = 0.994$). Higher concentration DSPE-PEG-Bi NPs showed higher PA signal values.

3.4. The CT and PAI Imaging In Vivo

To further demonstrate the CT capability of DSPE-PEG-Bi NPs in tumor-bearing mice, 200 μL DSPE-PEG-Bi NPs solution (10 mg/mL) were administered intravenously to obtain the imaging and the CT value of tumor. As shown in Fig. 4c, the 3D-MRP (Multiple Reuse Pattern) with coronal and axial CT imaging was conducted on tumor-bearing mice after 0.5 h, 1 h and 3 h injection of DSPE-PEG-Bi NPs, respectively. After injected 0.5 h, the spleen and liver exhibited obvious

contrast enhancement, and the enhancement continued for 3 h. Additionally, the CT value of tumor region was 225.7 Hu after 1 h injection (Fig. 4a), which was significant higher than pre-injection (0 h). The above results indicated that the DSPE-PEG-Bi NPs hold a great potential in CT enhancement in vivo.

In addition, given the excellent PAI efficacy of DSPE-PEG-Bi NPs in vitro, the capability of DSPE-PEG-Bi NPs for PAI enhancement in vivo was further investigated. The PAI imaging was collected by an Endra Nexus 128 PA system, following intravenous injection of 10 mg/mL DSPE-PEG-Bi NPs. As shown in Fig. 4d, obvious enhancement was detected in tumor region. Meanwhile, the PAI signal value in tumor region of mice (Fig. 4b), an obvious increasing from 0 to 958 after 1 h injection of DSPE-PEG-Bi NPs. As shown in Fig. 4d, the tumor region exhibited a weak signal before DSPE-PEG-Bi NPs injection, which could be due to the rich blood in tumor. Moreover, due to EPR effect, the PAI signal was still stronger than the signal of pre-injection, which could demonstrate the DSPE-PEG-Bi NPs had long residence time. Such excellent in vivo PAI performance indicated the potential of DSPE-PEG-Bi NPs as PAI contrast agent.

3.5. Cytotoxicity Study & the Photothermal Therapy Effect

Given the excellent performance in photothermal conversion, the DSPE-PEG-Bi NPs could be used as a promotional PTT-agent for tumor therapy. To further investigate the cytotoxicity and PTT efficacy of the DSPE-PEG-Bi, MTT assay and live/dead cell staining were studied though C6 cells or Cos-7 cells co-incubated with DSPE-PEG-Bi NPs. We firstly tested the cytotoxicity of DSPE-PEG-Bi NPs with different concentration (200, 100, 50, 25, 12.5, 6.25 mg/mL). At the present in Fig. 5a, whether co-incubation with C6 cells or Cos-7 cells, >80% C6 cells were alive even co-incubated with the relative higher concentration of 200 mg/mL DSPE-PEG-Bi NPs, which showed DSPE-PEG-Bi NPs
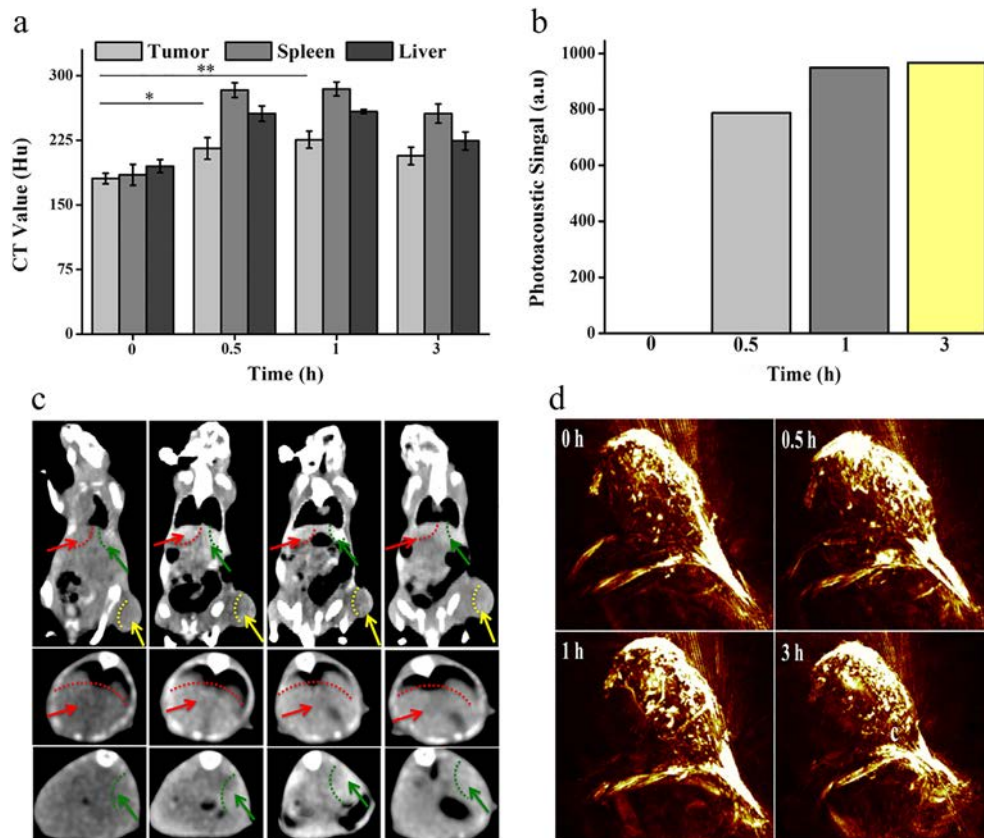

Fig. 4. a) The CT value of tumor, liver and spleen before and after injection. (*, $p < .05$; *, $p < .005$, $n = 3$) b) The PA value of tumor before and after injection. c) The CT imaging of mice liver (red arrow), spleen (green arrow) and tumor (yellow arrow)at different time. d) The PA imaging of tumor at different time. A dotted white line indicates the tumor region.
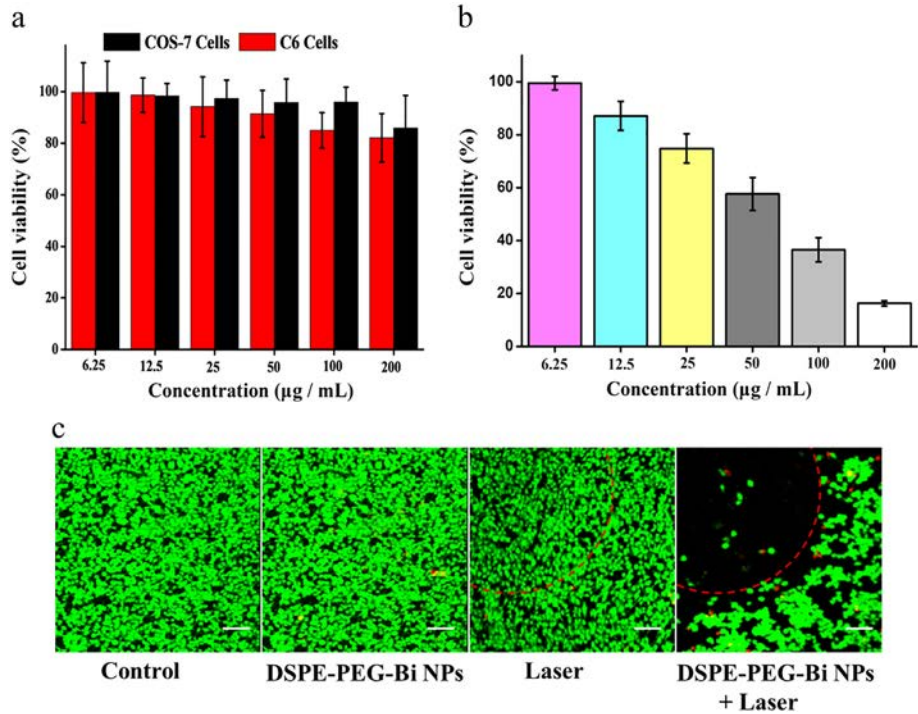
Fig. 5. a) C6 cells and Cos-7 cells viability of different DSPE-PEG-Bi NPs concentration after co-incubated 24 h. b) C6 cells viability of different DSPE-PEG-Bi NPs concentration after laser irradiation. c) Photothermal destruction of C6 cells after different treatment. A dotted red line indicates the laser illumination zone, the living cells were stained green and the dead cells were red. (Scale bar is 100 μm.)
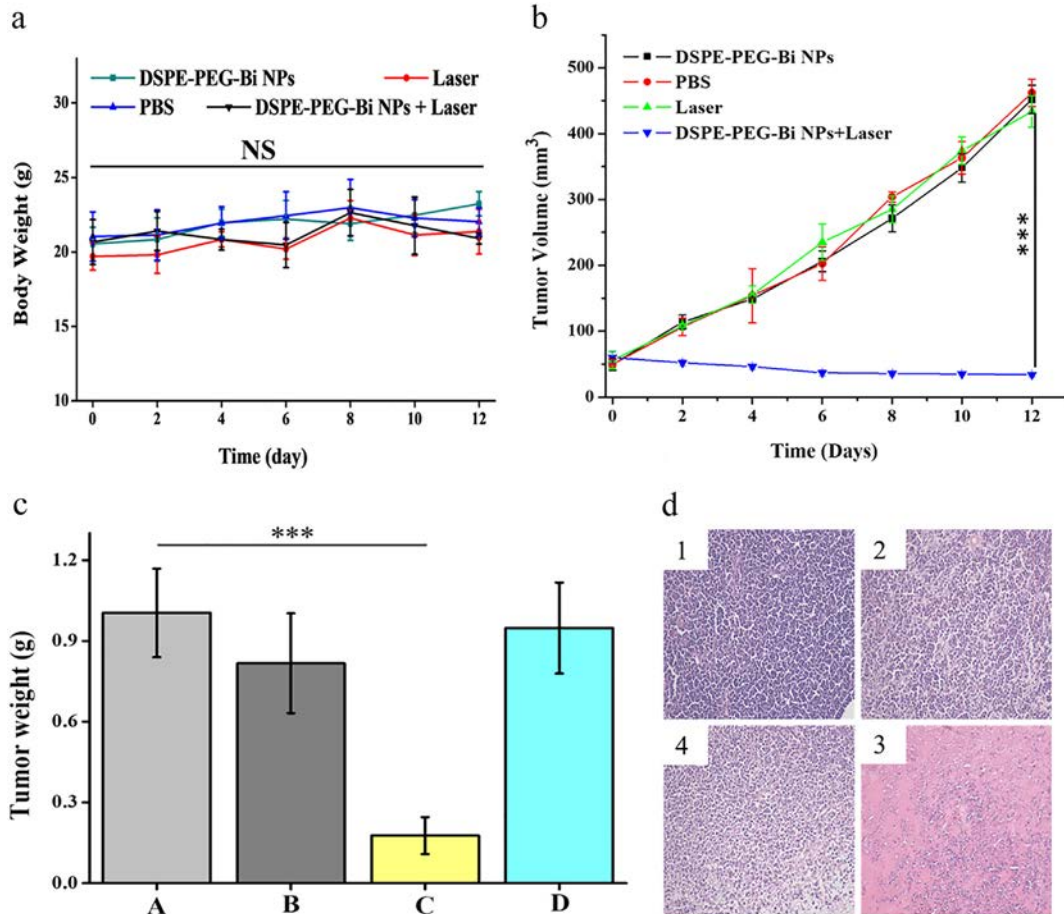

Fig. 6. a) The body weight and b) the tumor volume of tumor-bearing mice during 12 days with different treatments. c) The tumor weight at the last therapy. d) The images of H&E stained tumor regions with different treatments. 1. PBS only, 2. Laser only, 3. DSPE-PEG-Bi NPs only, 4. DSPE-PEG-Bi NPs + Laser. (Magnification: 200×) (NS, no significance; ***, p < .0005, n = 4).
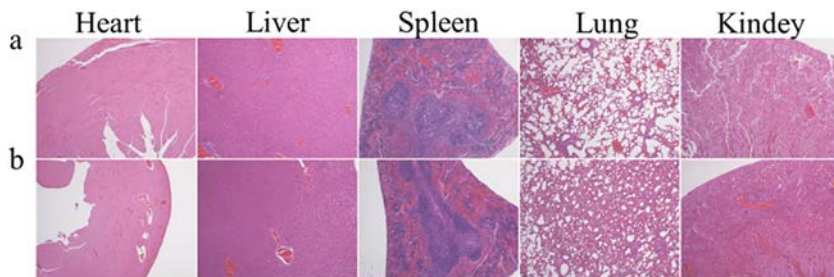
Fig. 7. Histology analysis of the major organs of mice after 12 days treatments. a) the group of DSPE-PEG-Bi NPs and irradiation. b) the group of PBS. (Magnification: 40×.)

exhibited no obvious cytotoxicity. In contrast, with 808 nm laser irradiation, the cell viabilities of C6 cells were decreased gradually with the concentration of DSPE-PEG-Bi NPs. As shown in Fig. 5b, >80% of C6 cells was killed with DSPE-PEG-Bi NPs (200 μg/mL) under 1 W/cm² irradiation, which demonstrated that the DSPE-PEG-Bi NPs had good NIR-induced phototoxicity for *in vitro* PTT.

Due to the high photothermal conversion efficiency of DSPE-PEG-Bi NPs, the photothermal ablation ability against C6 cells were observed by confocal microscopy (CM) with Calcein-AM/PI Double Stain (the living cells were stained green and the dead cells were stained red). C6 cells co-incubated with DSPE-PEG-Bi NPs were divided into four groups. As presented in Fig. 5c, the C6 cells of the three control groups were almost lighted up as green in the whole visual field. However, for the experiment group (DSPE-PEG-Bi NPs + laser), almost no C6 cells remained alive (the most dead cells were not stained due to floating) and a clear boundary appeared around the NIR irradiation zone, which was consistent with MTT assay results. In addition, some dead cells were found outside of irradiation zone, which may cause by the spreading of high temperature under irradiation. All the above *in vitro* results suggested that the DSPE-PEG-Bi NPs could be used as an encouraging PTT agent for further biomedical applications.

3.6. The Effect of Cancer Therapy

The excellent performance in CT/PA/PT imaging indicated that DSPE-PEG-Bi NPs could be served as a qualified theranostic for imaging targeted tumor diagnose and photothermal therapy both *in vitro* and *in vivo*. Here, the tumor size of mice with or without treatment was continuously observed for 12 days.. As shown in Fig. 6b, the final tumor volume was 34.09 ± 3.37 mm³ (n = 4), which was much smaller than the initial tumor volume (60.41 ± 8.25 mm³). This result indicated that during the whole observation period, the tumor growth of group which treated with DSPE-PEG-Bi NPs injection and 808 nm laser irradiation was significantly suppressed. However, a converse trend was observed in three groups from the C6 tumor growth curves of mice. The tumors volume in control groups was increased to exceed 400 mm³. And the relative tumor volume in three control groups was nearly 15 times larger than the treatment group at the last day. Similarly, Fig. 6c directly displayed that the tumor weight treated with DSPE-PEG-Bi NPs + irradiation was the smallest, which further confirmed obviously inhibition in tumor growth. Simultaneously, the body weight have no significant difference with different treatments (n = 4) (Fig. 6a),
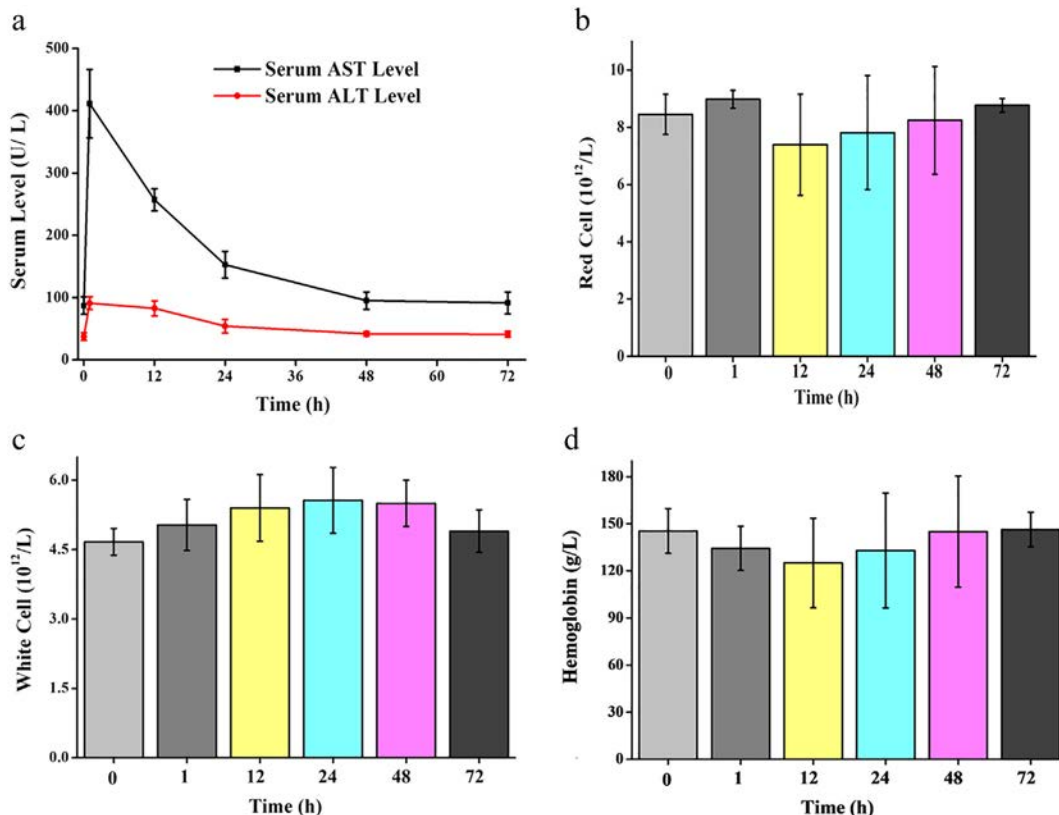

Fig. 8. a) The curve of liver function and (b-d) hematology data of mice sacrificed at different time (n = 3).

which demonstrated no obvious toxicity of different treatments. In addition, the biological effect of DSPE-PEG-Bi NPs was detected through histological analysis. As shown in Fig. 6d, tumors treated with DSPE-PEG-Bi NPs + irradiation showed the large area of necrosis and most of tumor cells were killed. Comparatively, tumor cells of the three control groups grew well after treatment. Meanwhile, no obviously damage was found in the main organs after treatment (Fig. 7). These results suggested that the DSPE-PEG-Bi NPs with NIR irradiation were beneficial in controlling the growth of initial tumors, which could destroy the tumors completely.

3.7. Liver Function and Blood Analysis

To further the safety of DSPE-PEG-Bi NPs *in vivo*, liver function and blood analysis were measured. As shown in Fig. 8a, alanine aminotransferase (ALT) and aspartate aminotransferase (AST) were back to normal quickly after an initial transient increase. The transient increase in ALT and AST levels in serum upon administration of DSPE-PEG-Bi NPs appears to be the general response of the body (Fig. 8a). It appears that the surge in enzyme activities seen in the animals during the initial hours following nanoparticle injection is partly the effect of the anesthetic agent used prior to injection, as a PBS injection also caused an increase in the liver AST and ALT level 37,38. The result was similar to Chen et.al [39]. Besides, as present in Fig. 8b-d, the blood panel measurement was revealed to be within reference ranges at each time. The results further confirmed that DSPE-PEG-Bi NPs could be application *in vivo* with good biocompatibility.

4. Conclusion

In summary, we have successfully developed a kind of multifunction and simple DSPE-PEG coated pure Bi NPs by an ultrasonic emulsification method, which could be used for both PA/CT imaging and photothermal therapy. With a 808 nm laser irradiation, the temperature of the DSPE-PEG-Bi NPs solution and tumor region increased to ~70 °C and ~50 °C, which showed the excellent photothermal performance of DSPE-PEG-Bi NPs. Moreover, DSPE-PEG-Bi NPs exhibited remarkable CT and PA contrast enhancement *via* the experiments *in vitro* and *in vivo*. Additionally, DSPE-PEG-Bi NPs with NIR laser irradiation could kill C6 cells and inhibit the growth of tumor obviously. Thus, this study suggests that the prepared DSPE-PEG-Bi NPs could be served as a multifunctional theranostic for CT/PA imaging and photothermal cancer therapy.

Conflicts of Interest

There are no conflicts to declare.

Acknowledgements

References

[1] Huang X, El-Sayed IH, Qian W, El-Sayed MA. J Am Chem Soc 2006;128:2115–20.
[2] Robinson JT, Tabakman SM, Liang Y, Wang H, Casalongue HS, Vinh D, et al. J Am Chem Soc 2011;133:6825–31.
[3] Maltzahn GV, Park JH, Agrawal A, Bandaru NK, Das SK, Sailor MJ, et al. Cancer Res 2009;69:3892–900.
[4] Jokerst JV, Lobovkina T, Zare RN, Gambhir SS. Nanomedicine 2011;6:715–28.
[5] Augustine S, Singh J, Srivastava M, Sharma M, Das A, Malhotra BD. Biomater Sci 2017;5:901–52.
[6] Leuenberger P, Ganscha S, Kahraman A, Cappelletti V, Boersema PJ, von Mering C, et al. Science 2017;355(6327):24.
[7] Riback JA, Katanski CD, Kear-Scott JL, Pilipenko EV, Rojek AE, Sosnick TR, et al. Cell 2017;168:1028–40.
[8] Liu B, Li C, Cheng Z, Hou Z, Huang S, Lin J. Biomater Sci 2016;4:890–909.
[9] Ming W, Da Z, Yongyi Z, Lingjie W, Xiaolong L, Jingfeng L. Nanotechnology 2015;26:115102.
[10] Liu J, Zheng X, Yan L, Zhou L, Tian G, Yin W, et al. ACS Nano 2016;12:696–707.
[11] Wang LV, Hu S. Science 2012;335:1458–62.
[12] Zemp RJ. Review of scientific instruments, vol. 77; 2006; 305–598.
[13] Mallidi S, Larson T, Tam J, Joshi PP, Karpiouk A, Sokolov K, et al. Nano Lett 2009;9:2825–31.
[14] Kircher MF, Zerda ADL, Jokerst JV, Zavaleta CL, Kempen PJ, Mittra E, et al. Nat Med 2013;18:829.
[15] Jing L, Liang X, Deng Z, Feng S, Li X, Huang M, et al. Biomaterials 2014;35:5814–21.
[16] Jin Y, Li Y, Ma X, Zha Z, Shi L, Tian J, et al. Biomaterials 2014;35:5795–804.
[17] Yang D, Ma P, Hou Z, Cheng Z, Li C, Lin J. Chem Soc Rev 2015;46:1416–48.
[18] Nilsson C, Barrios-Lopez B, Kallinen A, Laurinmäki P, Butcher SJ, Raki M, et al. Biomaterials 2013;34:8491–503.
[19] Wang J, Tan X, Pang X, Liu L, Tan F, Li N. ACS Appl Materi Inter 2016;8:24331.
[20] Cheng K, Kothapalli SR, Liu H, Koh AL, Jokerst JV, Jiang H, et al. J Am Chem Soc 2014;136:3560–71.
[21] Cui C, Gan L, Heggen M, Rudi S, Strasser P. Nat Mater 2013;12:765–71.
[22] Lee N, Choi SH, Hyeon T. Adv Mater 2013;25:2641–60.
[23] Ai K, Liu Y, Liu J, Yuan Q, He Y, Lu L. Adv Mater 2011;23:4886.
[24] T J, Alivisatos AP. Nano Lett 2006;6:2701–6.
[25] Peterson WL, Ciociola AA, Sykes DL, Mcsorley DJ, Webb DD. Aliment Pharmacol Ther 1996;10:251.
[26] Wong BCY, Wong WM, Wang WH, Fung FMY, Lai KC, Chu KM, et al. Gastroenterology 2001;15:403–9.
[27] Song G, Liang C, Gong H, Li M, Zheng X, Cheng L, et al. Adv Mater 2015;27:6110.
[28] Wu B, Lu ST, Yu H, Liao RF, Li H, Lucie Zafitatsimo BV, et al. Biomaterials 2018;159:37–47.
[29] Zha Z, Deng Z, Li Y, Li C, Wang J, Wang S, et al. Nanoscale 2013;5:4462.
[30] Cheng L, Liu J, Gu X, Gong H, Shi X, Liu T, et al. Adv Mater 2014;26:1886–93.
[31] Chen YJ, Xiao G, Wang TS, Ouyang QY, Qi LH, Ma Y, et al. Chemistry C 2011;115:10061–4.
[32] Z L, Y H, M C, KA H, X F, Y S, et al. Nanoscale 2016;8:16005.
[33] Wang S, Li X, Chen Y, Cai X, Yao H, Gao W, et al. Adv Mater 2015;27:2775–82.
[34] Maruyama K. Adv Drug Deliv Rev 2011;63:161.
[35] Thomson JW, Lawson G, O'Brien P, Klenkler R, Helander MG, Petrov S, et al. Adv Mater 2010;22:4395–400.
[36] Martinez L, Bernechea M, Arquer FPGD, Konstantatos G. Adv Ener Mater 2011;1:1029–35.
[37] Jiang X, Dai H, Leong KW, Goh SH, Mao HQ, Yang YY. J Gene Med 2006;8:477–87.
[38] Jain TK, Reddy MK, Morales MA, Leslie-Pelecky DL, Labhasetwar V. Mol Pharm 2008;5:316–27.
[39] Chen J, Yang XQ, Qin MY, Zhang XS, Xuan Y, Zhao YD. J Nanobiotechnol 2015;13:76.